small
www.small-journal.com

A White Light-Emitting Quantum Dot Complex for Single Particle Level Interaction with Dopamine Leading to Changes in Color and Blinking Profile

*Sabyasachi Pramanik, Satyapriya Bhandari, Uday Narayan Pan, Shilaj Roy, and Arun Chattopadhyay**

The interaction of the neurotransmitter dopamine is reported with a single particle white light-emitting (WLE) quantum dot complex (QDC). The QDC is composed of yellow emitting ZnO quantum dots (Qdots) and blue emitting $Zn(MSA)_2$ complex (MSA = *N*-methylsalicylaldimine) synthesized on their surfaces. Sensing is achieved by the combined changes in the visual luminescence color from white to blue, chromaticity color coordinates from (0.31, 0.33) to (0.24, 0.23) and the ratio of the exponents (α_{on}/α_{off}) of on/off probability distribution (from 0.24 to 3.21) in the blinking statistics of WLE QDC. The selectivity of dopamine toward ZnO Qdots, present in WLE QDC, helps detect ≈13 dopamine molecules per Qdot. Additionally, the WLE QDC exhibits high sensitivity, with a limit of detection of 3.3×10^{-9} M (in the linear range of 1–100 $\times 10^{-9}$ M) and high selectivity in presence of interfering biological species. Moreover, the single particle on–off bilking statistics based detection strategy may provide an innovative way for ultrasensitive detection of analytes.

1. Introduction

Colloidal semiconductor quantum dot (Qdot) single particles provide an important option for sensing molecule and phenomenon at the highest resolution using light as the probe.[1–12] However, the performance is significantly impeded by intermittency in photoluminescence referred to as blinking.[1–12] Chemical methods of suppression of blinking can also be considered to contain hint of the nature of the environment surrounding the emissive Qdot. Notably, the changes in the blinking statistics, especially the exponents of the on and/or off probability distribution,[1–15] in the presence of an analyte could also be considered a characteristic useful in sensing.

S. Pramanik, U. N. Pan, S. Roy, Prof. A. Chattopadhyay
Department of Chemistry
Indian Institute of Technology Guwahati
Guwahati 781039, Assam, India
E-mail: arun@iitg.ernet.in
Dr. S. Bhandari, Prof. A. Chattopadhyay
Centre for Nanotechnology
Indian Institute of Technology Guwahati
Guwahati 781039, Assam, India
The ORCID identification number(s) for the author(s) of this article can be found under https://doi.org/10.1002/smll.201800323.

DOI: 10.1002/smll.201800323

While there exists a vast literature on sensing of molecules using Qdots, the primary means that is used is the change in intensity of luminescence at a particular wavelength in the presence of the analyte.[16–26] Also, change in the wavelength of emission, when the two species interact, has also been utilized. Ratiometric sensing using emissions at two different wavelengths has also been preferred for a more quantitative analysis. However, a new option could also be thought of where the color of the white light-emitting (WLE) Qdot would change upon interaction with the analyte. We have recently introduced the functionalization of Qdots with inorganic complexes on their surface giving rise to emission due to all the components, namely, the Qdot and the surface complexes. This has given rise to the generation of WLE Qdot complex (QDC).[27–30] Similarly, starting with the WLE QDC one can have reaction/interaction with an analyte and observe the change in color visually more easily. This could also bring in a new way of sensing using singular QDC.

Herein, we report the fabrication of a new WLE QDC—based on the formation of blue-emitting complex of *N*-methylsalicylaldimine (MSA) with Zn^{2+}, that is, $Zn(MSA)_2$ on the surface of yellow emitting ZnO Qdot. We also report that the same QDC could be used for visual detection of the catecholamine neurotransmitter dopamine based on luminescence color change from white to blue (with associated change in the chromaticity coordinates) in the dispersion medium. Rapid detection and accurate quantification of dopamine is significant for practical clinical diagnosis and monitoring of patients afflicted with diseases, such as Parkinson's disease, Huntington's disease, and schizophrenia. Importantly, the same QDC could be used for sensing of dopamine at the level of single particle with the color change that could be recorded using confocal laser scanning microscopy (CLSM). Further, the on–off blinking rate (i.e., the ratio of the exponents) of the QDC changed to a higher value in the presence of the analyte. We observed that dopamine reacted with the QDC, possibly forming a new complex on the surface and lowering the emission quantum yield of the ZnO Qdot and without affecting the emission of the already present complex $Zn(MSA)_2$.

© 2018 WILEY-VCH Verlag GmbH & Co. KGaA, Weinheim

2. Results and Discussion

The details of the synthesis of ligand-free wurtzite ZnO Qdots, (following reported method),[30] MSA ligand, and WLE QDC nanocomposite are described in the Experimental Section. Digital photographs (captured under a 350 nm light from a spectrofluorimeter) showed that the treatment of MSA ligand to presynthesized ZnO Qdots led to the change in their luminescence color from yellow to white due to the formation of QDC (**Figure 1**A). The QDC (at $\lambda_{ex} \approx 350$ nm) exhibited a new blue emission peak at 440 nm (due to the electronic transition from the highest occupied molecular orbital to the lowest unoccupied molecular orbital of surface $Zn(MSA)_2$ complex)[30]—in addition to the pristine broad yellow emission (centered at 550 nm) of ZnO Qdot (originating from surface trap states of the Qdots)[30] (Figure 1B). Similarly, a new peak at 318 nm appeared (indicative of the formation of $Zn(MSA)_2$ complex), along with the band edge of ZnO Qdots at 350 nm, for QDC in the absorption spectrum (Figure S1, Supporting Information). No significant change was observed in the excitation spectrum (at $\lambda_{em} \approx 550$ nm) of the ZnO Qdots, following addition of MSA (Figure S2, Supporting Information). Furthermore, QDC exhibited the chromaticity coordinates of (0.31, 0.33), which is for near to perfect white light emitter, while (0.36, 0.43) chromaticity coordinates were observed for only ZnO Qdots (Figure 1C). The results clearly indicated the WLE nature of QDC. It is to be mentioned here that the concentration of MSA ligand was chosen based on the chromaticity coordinates near to perfect white light (0.33, 0.33)[27–30] and it was found that the optimum amount of MSA needed to generate white light from ZnO Qdots (with absorbance of 0.11 at 350 nm) was 9.9×10^{-6} M (Figure S3, Table S1, Supporting Information).

The photoluminescence quantum yield (PLQY; measured with respect to quinine sulphate) of the WLE QDC was found to be 2.4%, while as such ZnO Qdots showed 1.2% of PLQY (Table S2, Supporting Information). Additionally, QDC exhibited average emission lifetimes of 4.1 ns (for emission at 440 nm) and 38.0 ns (for emission at 550 nm) and no significant change was observed with respect to the average lifetime of the ZnO Qdots ($\lambda_{em} \approx 550$ nm, $\tau_{av} = 38.8$ ns), following MSA addition (Figure S4, Table S3, Supporting Information). Importantly, the preservation of the crystalline integrity (in terms of size, diffraction pattern, and lattice fringe)[30] of the wurtzite ZnO, following complexation with MSA, clearly indicated successful formation of WLE QDC (Figure S5, Supporting Information). Furthermore, the stability of the luminescence (at $\lambda_{ex} \approx 350$ nm; probed up to 48 h) and the cell viability (after 24 h) assay of the different concentrations of colloidal WLE QDC indicated their colloidal stability and no apparent toxicity and thus to their application potential, especially in making biosensors (Figure S6, Supporting Information).

When viewed under a confocal laser scanning microscope (using 355 nm laser), QDC exhibited intense color owing to blue and yellow emissions (due to the presence of two emitting species $Zn(MSA)_2$ complex and ZnO Qdots) and the merged image clearly supports the bright white light nature to the QDC (Figure 1D). The single particle nature of WLE QDC (deposited on a glass cover slip) was demonstrated based on the blinking activity, that is, time-dependent alteration between on state (emitting state) and off state (dark state) using CLSM under superresolution. This is a primary signature, of single luminescent nanocrystals, which distinguishes them from multiple nanocrystals.[1–15] Figure 1E shows the superresolution representative image of the white colored particles as obtained from Figure 1D (iii). Corresponding blinking activity of a single WLE QDC was recorded for the marked particle. Movie S1 (Supporting Information) clearly demonstrates the blinking activity of the WLE QDC and thus supports the single particle nature. Importantly, WLE QDC exhibited square wave shaped on–off blinking,[7,15] in time varying fluorescence intensity profile (Figure 1F; blinking profile was recorded for the particle, which was shown in Movie S1 in the Supporting Information). This is also in support of the single particle nature of the WLE QDC and ruled out the possibility of observation of multiple particles (which generally exhibit flickering in-between on and dim states, as shown in Figure S7, Supporting Information).[7,31–36] Histogram (based on the blinking data obtained from Figure 1F) showed the occurrence of more number of on states, compared to off states, in the blinking profile of the WLE QDC and the on/off occurrence ratio was found to be 8.44 (Figure 1G). In our case, the probability distributions of the events (on and off) could be fitted well by a truncated power law[31–36] through a log–log plot extracted from the obtained data points for 40 single particles (Figure 1H,I), the details of which are described in the Experimental Section. It is to be mentioned here that the exponent of the power-law distribution (known as α_{on} and α_{off}) of the on and off events is an important parameter with regard to the luminescence behavior of a blinking single nanocrystal.[1–15,31–36] Hence, any chemical reaction or physical interaction that alters the emission characteristics of a single nanocrystal may lead to change in the exponents (α_{on} and α_{off}) and their ratio (α_{on}/α_{off}) in the blinking statistics.[13,31,37] In other words, the exponents (α_{on} and α_{off}) and their ratio (α_{on}/α_{off}) of a blinking single nanocrystal can be considered useful in describing the presence of any chemically reactive analyte on the surface and thus have important consequences in sensing application.[13,31,37] Importantly, the value of the exponent (α_{on}) of the on-duration probability distribution (P_{on}) was found to be lesser compared to the exponent (α_{off}) of the off-duration probability distribution (P_{off}) for single WLE QDC ($\alpha_{on} = 0.42 \pm 0.04 < \alpha_{off} = 1.75 \pm 0.03$; Figure 1H,I, Table S4, Supporting Information). This was calculated using a fixed frame size of 64×64 μm^2 and binning time of 27 ms[35,36] with excitation power of 63 mW for a time duration of 27 s for each single particle. This result clearly supported the presence of more number of on states in comparison to off states in the blinking behavior of single WLE QDC, with a (α_{on}/α_{off}) ratio of 0.24.

Importantly, the digital photographs (captured with an excitation of 350 nm light from a spectrofluorimeter) of WLE QDC upon dopamine addition clearly showed the visual color changes from white to blue (**Figure 2**A). The sequential addition of dopamine (in the range of $6.6 \times 10^{-9} - 1.2 \times 10^{-6}$ M) to the WLE QDC nanocomposite (in ethanol; having absorbance of 0.11 at 350 nm) led to the gradual quenching in the emission intensity at 550 nm, while no significant change was observed with respect to the other emission intensity at 440 nm of the WLE QDC (Figure 2B). Further, the change in the chromaticity

© 2018 WILEY-VCH Verlag GmbH & Co. KGaA, Weinheim

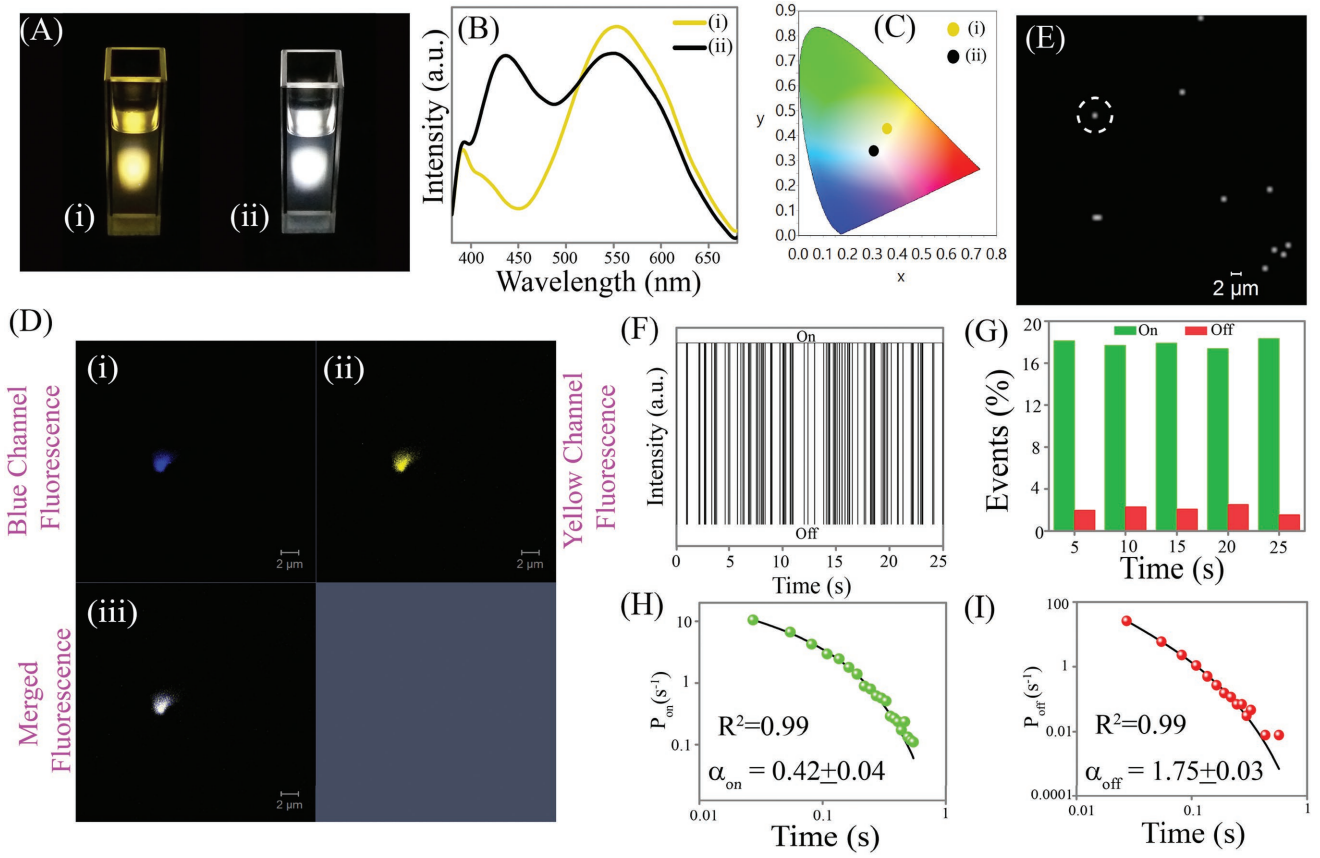

Figure 1. A) Photographs (digitally captured under 350 nm light from a spectrofluorimeter), B) emission spectra ($\lambda_{ex} \approx 350$ nm), and C) corresponding chromaticity color coordinates in CIE diagram of the ethanolic dispersion of (i) ligand-free ZnO Qdots and (ii) WLE QDC. D) Confocal laser scanning microscopic images (scale bar 2.0 μm) of WLE QDC recorded in (i) blue and (ii) yellow emission channels, and (iii) their merged version. E) Superresolution confocal laser scanning microscopic image of WLE QDC (scale bar 2.0 μm; with respect to the area as obtained in the merged portion of panel (D) (iii)). F) Representative time-dependent blinking profile of WLE QDC (related to the encircled particle shown in the panel (E) and Movie S1 in the Supporting Information). G) Histogram of proportion of on and off states of a Qdot present in WLE QDC (with respect to the blinking profile mentioned in panel (F)). H,I) Corresponding probability densities of on-states ($P_{on}(t)$) and off-states ($P_{off}(t)$) for single Qdots (present in WLE QDC). The data were obtained by using frame size of 64 × 64 μm^2, binning time of 27 ms, excitation power of 63 mW, and for a time duration of 27 s. The 355 nm laser was used to excite the samples.

color coordinates from (0.31, 0.33) to (0.24, 0.23) of WLE QDC nanocomposite, upon dopamine addition, clearly supported the visual color change from white to blue (Figure 2C, Table S5, Supporting Information). The quenching effect of dopamine on the emission intensity, at 550 nm, of WLE QDC was demonstrated by Stern–Volmer equation[20–26] (Figure S8, Supporting Information). Figure S8 (Supporting Information) depicts an excellent linear relationship between I_o/I and the concentration of dopamine in the range of 1–100 × 10^{-9} M, with K_{sv} value of 3.4 × 10^6 M^{-1} and correlation coefficient of 0.98. The limit of detection of dopamine was found to be 3.3 × 10^{-9} M. Similarly, the decrease in the average lifetime (with respect to the emission at 550 nm) of WLE QDC, following dopamine addition, clearly demonstrated the dynamic quenching behavior in the linear range of 1–100 × 10^{-9} M (Figure S9, Table S6, Supporting Information). Further, the selectivity of the luminescence of WLE QDC nanocomposite toward dopamine was confirmed by incubating them with interfering biomolecules, such as uric acid, cysteine (Cys-S—H), tryptophan (Trp), glutamic acid (Glu), arginine (Arg), phenylalanine (Phe), tyrosine (Tyr), and aspartic acid (Asp) at higher amounts (2.0 × 10^{-6} M) compared to dopamine (1.2 × 10^{-6} M) (Figure S10, Supporting Information). The results showed no noticeable effects on the yellow emission of the WLE QDC nanocomposite and thus clearly indicated the high selectivity of WLE QDC toward dopamine in the presence of mentioned interfering molecules.

Additionally, no significant change was observed in the absorption spectrum of the WLE QDC nanocomposite, following dopamine addition (Figure S11, Supporting Information). The WLE QDC showed quenching in the excitation intensity at 350 nm, when emission was probed at 550 nm. However, there was no significant change in the excitation spectrum of WLE QDC, at $\lambda_{em} \approx 440$ nm (Figure S2, Supporting Information). The selectivity of reaction of dopamine with ZnO Qdots over Zn(MSA)$_2$ complex was further confirmed by observing similar quenching in the luminescence intensity of only ZnO Qdots (at 550 nm) (Figure S12, Supporting Information). No noticeable change in the luminescence intensity of only Zn(MSA)$_2$ complex (at 440 nm) upon dopamine addition was observed (Figure S12, Supporting Information). The results

© 2018 WILEY-VCH Verlag GmbH & Co. KGaA, Weinheim

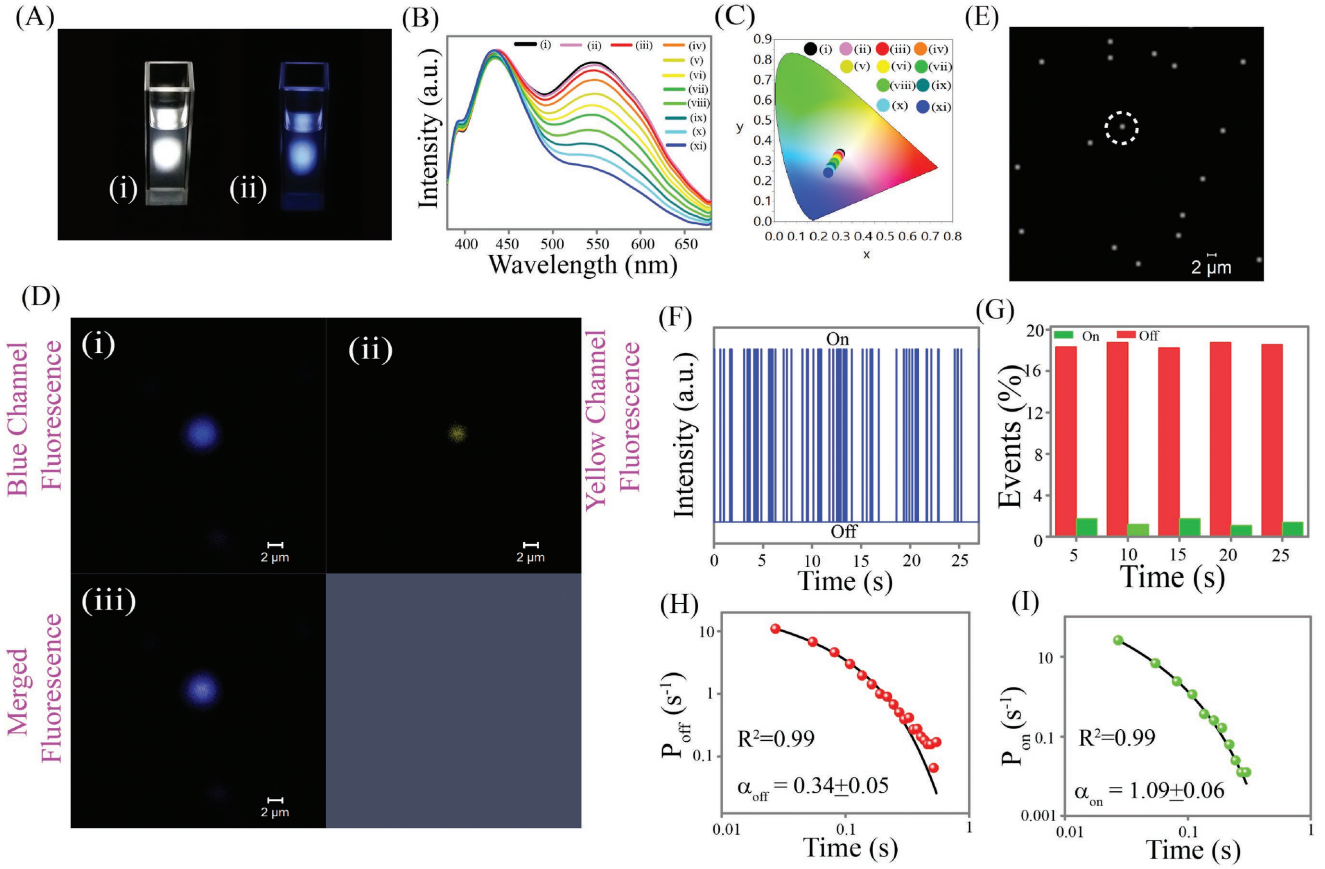

Figure 2. A) Photographs (digitally captured under 350 nm light from a spectrofluorimeter) of (i) WLE QDC nanocomposite (with absorbance of 0.11 fixed at 350 nm) and (ii) dopamine added to WLE QDC nanocomposite dispersions. B) Emission spectra ($\lambda_{ex} \approx 350$ nm) and C) changes in chromaticity color coordinates in CIE diagram of (i) 0.0, (ii) 6.6, (iii) 13.3, (iv) 26.6, (v) 46.4, (vi) 72.8, (vii) 99.0, (viii) 196.0, (ix) 322.0, (x) 625.0, and (xi) 1176.5 × 10^{-9} M dopamine added to WLE QDC nanocomposite. D) Confocal laser scanning microscopic images of dopamine treated WLE QDC (scale bar 2.0 μm) recorded using (i) blue and (ii) yellow emission channels and (iii) their merged version. E) Superresolution confocal laser scanning microscopic image (scale bar 2.0 μm; with respect to the area as obtained in the merged portion of panel (D) (iii)) of dopamine added WLE QDC. F) Representative time-dependent blinking profile of dopamine added WLE QDC (which is related to the encircled particle shown in panel (E) and Movie S2 in the Supporting Information). G) Histogram of proportion of on and off states of a Qdot (present in dopamine added WLE QDC) with respect to the blinking profile mentioned in panel (F). H,I) Corresponding probability density of off-states ($P_{off}(t)$) and on-states ($P_{on}(t)$) for single Qdots (present in dopamine-added WLE QDC). The data were obtained by using frame size of 64 × 64 μm^2, binning time of 27 ms, excitation power of 63 mW, and for a time duration of 27 s. The 355 nm laser was used to excite the samples.

indicated that the yellow emission of the WLE QDC nanocomposite was sensitive to dopamine, compared to the blue emission, in the liquid medium. Furthermore, the preservation of the crystalline integrity (in terms of size and lattice fringe) of wurtzite ZnO Qdots[30] in WLE QDC nanocomposite— following interaction with dopamine —was confirmed by transmission electron microscope (TEM) and X-ray diffraction (XRD) analyses (Figure S5, Supporting Information).

Notably, when dopamine reacted with WLE QDC, the representative CLSM image showed that the intensity of the particle in the yellow channel became weak, while no significant change was observed in the blue channel (Figure 2D). Thus, the merged image of dopamine added WLE QDC exhibited blue color upon reacting with dopamine (Figure 2D-iii). However, a negligible white shade was noticed in the center of the merged CLSM image (Figure 2D-iii). This may be due to the presence of partial yellow luminescence of ZnO Qdot, which was not completely quenched when a fixed number of dopamine molecules reacted with WLE QDC. The result, however, demonstrated the color change from white to blue of a WLE QDC following interaction with dopamine. This further supported the observed luminescence color change from white to blue of WLE QDC upon dopamine addition. Figure 2E shows the superresolution representative image of the blue color particles as obtained from Figure 2D (iii). Corresponding blinking of a single WLE QDC, following dopamine addition, was recorded for the marked particle. Movie S2 (Supporting Information) clearly demonstrates the blinking of the dopamine added WLE QDC. Significantly, as dopamine reacted with WLE QDC, the ratio of the on/off states, in the time varying blinking intensity profile changed from 8.44 to 0.07 (Figure 2F,G; as shown in Movie S2, Supporting Information). Importantly, upon dopamine addition to single WLE QDC, the value of α_{on} increased from 0.42 ± 0.04 to 1.09 ± 0.06, while the value of α_{off} decreased from 1.75 ± 0.03 to 0.34 ± 0.05 (Figure 2H,I, Table S4, Supporting Information). The results were obtained by fitting the data points to truncated power

© 2018 WILEY-VCH Verlag GmbH & Co. KGaA, Weinheim

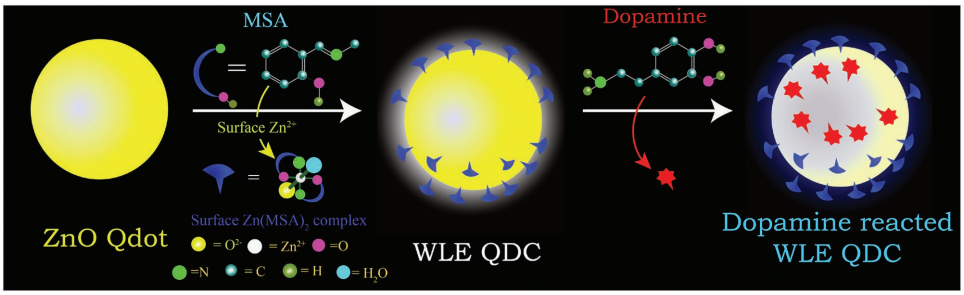

Scheme 1. Schematic representation of the formation of WLE QDC from yellow emitting ZnO Qdot, following complexation with MSA and thus the use of single particle WLE QDC for the ultrasensitive detection of dopamine based on the selective quenching of the yellow emission compared to blue emission.

law[31–36] using a log–log plot while considering the blinking profile of 40 single particles under same experimental condition. That is the conditions were similar to those used for WLE QDC (frame size 64 × 64 μm^2, binning time 27 ms,[35,36] excitation power 63 mW, time duration of 27 s). The results indicated the presence of higher numbers of off states compared to on states in the blinking profile of dopamine added WLE QDC and supported the preservation of single particle nature of WLE QDC, even after reaction with dopamine. Interestingly, the changes in the value of (α_{on}/α_{off}) ratio from 0.24 to 3.21 helped to detect ≈13 number of dopamine molecules by Qdot (present in WLE QDC) at the single particle level (Table S4, Supporting Information). The details of the calculation performed by combining the obtained results from atomic absorption and size analysis are described in Figure S13 in the Supporting Information. On the other hand, the value of (α_{on}/α_{off}) ratio changed from 0.55 to 3.52 when dopamine (with same concentration, which was used for WLE QDC) was added to only ZnO Qdots (Figure S14, Table S7, Supporting Information). This is in further support of the observation of selective reactivity of dopamine with ZnO Qdots compared to $Zn(MSA)_2$ complexes, present in WLE QDC. Additional movies (Movies S3–S4, Supporting Information) and corresponding CLSM images (Figure S15, Supporting Information) are included as supporting evidences to demonstrate the reproducibility of the single particle nature of WLE QDC and the presented concept. Hence, the reported strategy based on the changes in the on–off blinking statistics, visual luminescence color (from white to blue), and chromaticity of a single particle WLE QDC is a new, simple, and cost-effective method, for the detection of dopamine. This is different in comparison to other reported strategies, wherein no changes in the visual luminescence color and chromaticity were observed since only quenching of emission of Qdots was studied,[20–26] the details of which are summarized in Table S8 in the Supporting Information.

Scheme 1 illustrates a schematic representation of the formation of WLE QDC following complexation on the surface of ZnO Qdots (using MSA as the complexing agent). The scheme also represents the use of single particle WLE QDC for the ultrasensitive detection of dopamine, based on the selective chemical interaction with ZnO Qdots, compared to $Zn(MSA)_2$ complex. The electron transfer from photoexcited ZnO Qdots to their surface adsorbed oxidized dopamine (i.e., the in situ formation of quinone, which usually acts as an electron quencher, in the alkaline solution as is case here) present in WLE QDC through noncovalent hydrogen bonding interactions with surface hydroxyl ligands of ZnO Qdots,[18–26,38,39] may be one of the reasons for selective quenching of yellow emission of WLE QDC following dopamine addition. This was further supported by the results obtained when the quenching of yellow emission of WLE QDC following the addition of benzoquinone (which is a well-known electron quencher) was observed (Figure S16, Supporting Information). Additionally, the formation of nonfluorescent Zn-dopamine complex, which also acts as quencher of the emission of ZnO Qdots, via the chelating ability of the catechol part of dopamine toward surface free Zn^{2+} ions of WLE QDC may be the other reason for the observed selective quenching of yellow emission of ZnO Qdots, present in WLE QDC.[40] It may be mentioned here that complexation reaction that was performed to get white light from ZnO Qdots following reaction with MSA might not have resulted in the complete coverage of the surface of the Qdots. This further helped reaction of the free Zn^{2+} ions with dopamine.

3. Conclusion

In conclusion, a highly sensitive and selective strategy for the visual detection of dopamine, following the change in luminescence color of WLE QDC from white to blue with corresponding chromaticity change from (0.31, 0.33) to (0.24, 0.23), has been developed. Sensing at the level of single Qdot particle (present in WLE QDC) was demonstrated using the time-dependent changes in the on/off states of the blinking statistics of a single particle WLE QDC. Importantly, the changes in the value of (α_{on}/α_{off}) ratio from 0.24 to 3.21 and the on/off occurrence ratio 8.44 to 0.07 of single particle WLE QDC helped to detect ≈13 number of dopamine molecules. Additionally, the limit of detection of dopamine was found to be 3.3 × 10^{-9} M (using spectrofluorimeter). The results presented herein might propel new research in biomolecular sensing at the level of single particle using blinking as an important tool.

4. Experimental Section

Chemicals: Zinc acetate dihydrate (Merck), potassium hydroxide (KOH, Merck), salicylaldehyde (Sigma-Aldrich), 1 M methyl amine in methanol (Sigma-Aldrich), dopamine hydrochloride (Sigma-Aldrich),

© 2018 WILEY-VCH Verlag GmbH & Co. KGaA, Weinheim

quinine sulfate (Fluka, USA), sulphuric acid (Merck, India), benzoquione (Sigma-Aldrich), cysteine (Sigma-Aldrich), tryptophan (Sigma-Aldrich), arginine (Sigma-Aldrich), phenyl alanine (Sigma-Aldrich), glutamic acid (Sigma-Aldrich), aspartic acid (Sigma-Aldrich), tyrosine (Sigma-Aldrich), and uric acid (Sigma-Aldrich) and ethanol (Tedia) were procured and used directly without any purification.

Synthesis of Wurtzite ZnO Qdots: ZnO Qdots were synthesized, following a reported process,[30,41] with the use of ethanol as solvent. Briefly, under vigorous stirring at 25 °C, 2.0 mL 0.5 M KOH (dissolved in ethanol) was added dropwise to a 50.0 mL ethanolic solution of zinc acetate having concentration of 5.0×10^{-3} M and the resulting mixture, of milky white color, was kept for half an hour. Then, the resulting reaction mixture was centrifuged with a speed of 25 000 rpm for 15 min and the so obtained pellet was washed with ethanol (in order to remove excess unreacted salts). The same cycle was repeated and the final pellet was dispersed in 50.0 mL of ethanol for further experiments.

Synthesis of MSA Ligand: A reported condensation reaction between salicyaldehyde and methylamine was followed to synthesize MSA.[30,42,43] In brief, 2 mmol of methylamine was added dropwise to the solution of 2.0 mmol of salicylaldehyde in 20.0 mL methanol and the resulting mixture, of yellow color, was allowed to stir for 4 h at 25 °C. The column chromatographic technique was used to purify the product (MSA).

Synthesis of WLE QDC: The luminescence (under spectrofluorimeter) and chromaticity (in CIE-1931 diagram) were monitored to get optimum amount of MSA (in ethanol) needed to generate white light from 3.0 mL of ZnO Qdots (in ethanol: with absorbance of 0.10 at an excitation wavelength of 350 nm). The 1.0×10^{-3} M MSA was sequentially added to the ethanolic dispersion of ZnO Qdots (having absorbance of 0.10 at 350 nm) at 25 °C. The optimum amount of MSA was found to be of 9.9×10^{-6} M. The resulting mixture, obtained from the treatment of 9.9×10^{-6} M MSA to 3.0 mL ZnO Qdots, was centrifuged, with a speed of 25000 rpm for 15 min. Then, the so obtained pellet was repeatedly washed with ethanol and finally redispersed in same amount of ethanol. The dispersion and corresponding solid form (obtained from centrifugation and drying at room temperature) of the QDC were used for further experiments.

Cell Viability Assay: For cell viability assay, 10^4 human embryonic kidney (HEK 293) cells (which were procured from National Center for Cell Sciences, Pune, India and cultured in Dulbecco's modified Eagle's medium, supplemented with 10% (v/v) fetal bovine serum, penicillin (50 units mL^{-1}), and streptomycin (50 mg mL^{-1}) and maintained in 5% CO_2 humidified incubator at 37 °C) per well were seeded in a 96 well microplate and left for overnight for proper growing. Then, the fresh media containing varying concentrations of WLE QDC (1.6–33.3 μg mL^{-1}), following removal of the old medium, were added to the cells and incubated for 24 h. Finally, the 3-(4,5-dimethylthiazol-2-yl)-2,5-diphenyltetrazolium bromide-based cell viability assay was performed and the Bio-Rad 680 microplate reader was used to monitored the absorbance at wavelength 550 nm.

Confocal Microscopic Measurements and Blinking Analysis: Confocal imaging and single particle experiment of WLE QDC and dopamine added WLE QDC were performed by depositing the as-prepared dispersion (which was obtained from the treatment of 9.9×10^{-6} M MSA to 3.0 mL ZnO Qdots with absorbance of 0.10 at 350 nm at 25 °C) of the materials on a glass cover slip. Imaging and blinking analysis of the samples were carried out using Zeiss LSM-880 confocal laser scanning microscope, equipped with a 355 nm diode-pumped solid-state UV laser (63 mW) for excitation and Plan-Apochromat, 63x/1.40, oil-immersion objective for imaging. The resulting fluorescence data of different channel images and single particle experiments were collected through the GaAsP detector and Airyscan detector, respectively. The blinking profile and video were recorded in acquisition mode under super resolution with 64×64 μm^2 frame size and by using binning time of 27 ms,[35,36] with excitation power of 63 mW for a time duration of 27 s. The so obtained images and data were analyzed by ZEN black software.

Instruments: Rigaku TTRAX III X-ray diffractometer and TEM (JEOL JEM 2100F, maximum accelerating voltage 200 kV) were used to analyze the morphology and size of the samples. TEM and inverse fast Fourier transform analyses were done by using Gatan Digital Micrograph software. HORIBA Jobin Yvon FluoroMax-4 spectrofluorimeter and Perkin Elmer LAMBDA 750 UV–vis–near-infrared (NIR) spectrophotometer were used to record the luminescence and absorbance of the samples, respectively. Life-Spec-II spectrofluorimeter (Edinburgh Instrument, using 336 nm light emitting diode (LED) source and Pico Quant 375 nm laser source) was used to record the time-resolved photoluminescence measurements and FAST software was used to analyze the time-resolved spectra. CIE-1931 color space of the OSRAM color calculator was used to calculate the chromaticity of the samples. Atomic absorption spectrophotometer (Varian AA240FS model) was used to find the concentration of metal ions. LSM 880 confocal laser scanning microscope (Zeiss) was used to record the single particle behavior of the solid samples (deposited on a glass cover slip) using 355 nm laser excitation.

Supporting Information

Supporting Information is available from the Wiley Online Library or from the author.

Acknowledgements

The authors thank the Department of Electronics and Information Technology (no. 5(9)/2012-NANO (Vol. II)) Government of India for providing funding. Assistance from Srestha Basu, Ayan Pal, CIF, and Department of Physics (for XRD facility under DST-FIST programme—SR/FST/PII-020/2009), IIT Guwahati is acknowledged here.

Conflict of Interest

The authors declare no conflict of interest.

Keywords

complexation reactions, quantum dots, sensing, single particle, white light

Received: January 24, 2018
Revised: February 19, 2018
Published online:

[1] A. L. Efros, D. J. Nesbitt, *Nat. Nanotechnol.* **2016**, *11*, 661.
[2] C. Galland, Y. Ghosh, A. Steinbruck, M. Sykora, J. A. Hollingsworth, V. I. Klimov, H. Htoon, *Nature* **2011**, *479*, 203.
[3] D. Bhatia, S. Arumugam, M. Nasilowski, H. Joshi, C. Wunder, V. Chambon, V. Prakash, C. Grazon, B. Nadal, P. K. Maiti, *Nat. Nanotechnol.* **2016**, *11*, 1112.
[4] A. L. Routzahn, P. K. Jain, *Nano Lett.* **2015**, *15*, 2504.
[5] Y. F. Chen, J. Vela, H. Htoon, J. L. Casson, D. J. Werder, D. A. Bussian, V. I. Klimov, J. A. Hollingsworth, *J. Am. Chem. Soc.* **2008**, *130*, 5026.
[6] B. Omogo, F. Gao, P. Bajwa, M. Kaneko, C. D. Heyes, *ACS Nano* **2016**, *10*, 4072.
[7] B. Scholl, H. Y. Liu, B. R. Long, O. J. T. McCarty, T. O'Hare, B. J. Druker, T. Q. Vu, *ACS Nano* **2009**, *3*, 1318.
[8] J. Zhou, Q.-x. Wang, C.-y. Zhang, *J. Am. Chem. Soc.* **2013**, *135*, 2056.

© 2018 WILEY-VCH Verlag GmbH & Co. KGaA, Weinheim

[9] X. Michalet, F. Pinaud, T. D. Lacoste, M. Dahan, M. P. Bruchez, A. P. Alivisatos, S. Weiss, *Single Mol.* **2001**, *2*, 261.
[10] H. Qin, R. Meng, N. Wang, X. Peng, *Adv. Mater.* **2017**, *29*, 1606923.
[11] F. Gao, P. Bajwa, A. Nguyen, C. D. Heyes, *ACS Nano* **2017**, *11*, 2905.
[12] C. Galland, Y. Ghosh, A. Steinbrück, J. A. Hollingsworth, H. Htoon, V. I. Klimov, *Nat. Commun.* **2012**, *3*, 908.
[13] C. K. De, T. Routh, D. Roy, S. Mandal, P. K. Mandal, *J. Phys. Chem. C* **2018**, *122*, 964.
[14] S. R. Opperwall, A. Divakaran, E. G. Porter, J. A. Christians, A. J. Den Hartigh, D. E. Benson, *ACS Nano* **2012**, *6*, 8078.
[15] K. M. Fichter, M. Flajolet, P. Greengard, T. Q. Vu, *Proc. Natl. Acad. Sci. USA* **2010**, *107*, 18658.
[16] B.-R. Li, Y.-J. Hsieh, Y.-X. Chen, Y.-T. Chung, C.-Y. Pan, Y.-T. Chen, *J. Am. Chem. Soc.* **2013**, *135*, 16034.
[17] Y. Jie, N. Wang, X. Cao, Y. Xu, T. Li, X. Zhang, Z. L. Wang, *ACS Nano* **2015**, *9*, 8376.
[18] R. Khatchadourian, A. Bachir, S. J. Clarke, C. D. Heyes, P. W. Wiseman, J. L. Nadeau, *J. Biomed. Biotechnol.* **2007**, *2007*, 1.
[19] J. J. Van Dersarl, A. Mercanzini, P. Renaud, *Adv. Funct. Mater.* **2015**, *25*, 78.
[20] X. Zhou, A. Wang, C. Yu, S. Wu, J. Shen, *ACS Appl. Mater. Interfaces* **2015**, *7*, 11741.
[21] D. Diaz-Diestra, B. Thapa, J. Beltran-Huarac, B. R. Weiner, G. Morell, *Biosens. Bioelectron.* **2017**, *87*, 693.
[22] X. Zhou, P. Ma, A. Wang, C. Yu, T. Qian, S. Wu, J. Shen, *Biosens. Bioelectron.* **2015**, *64*, 404.
[23] S. Liu, F. Shi, X. Zhao, L. Chen, X. Su, *Biosens. Bioelectron.* **2013**, *47*, 379.
[24] D. Zhao, H. J. Song, L. Y. Hao, X. Liu, L. C. Zhang, Y. Lv, *Talanta* **2013**, *107*, 133.
[25] M. Shamsipur, M. Shanehasz, K. Khajeh, N. Mollania, S. H. Kazemi, *Analyst* **2012**, *137*, 5553.
[26] Q. Mu, H. Xu, Y. Li, S. J. Ma, X. H. Zhong, *Analyst* **2014**, *139*, 93.
[27] S. Pramanik, S. Bhandari, S. Roy, A. Chattopadhyay, *J. Phys. Chem. Lett.* **2015**, *6*, 1270.
[28] S. Bhandari, S. Pramanik, R. Khandelia, A. Chattopadhyay, *ACS Appl. Mater. Interfaces* **2016**, *8*, 1600.
[29] S. Pramanik, S. Bhandari, A. Chattopadhyay, *J. Mater. Chem. C* **2017**, *5*, 7291.
[30] S. Roy, S. Pramanik, S. Bhandari, A. Chattopadhyay, *Langmuir* **2017**, *33*, 14627.
[31] B. Li, G. F. Zhang, Z. Wang, Z. J. Li, R. Y. Chen, C. B. Qin, Y. Gao, L. T. Xiao, S. T. Jia, *Sci. Rep.* **2016**, *6*, 32662.
[32] Y. J. Bae, N. A. Gibson, T. X. Ding, A. P. Alivisatos, S. R. Leone, *J. Phys. Chem. C* **2016**, *120*, 29484.
[33] C. H. Crouch, O. Sauter, X. Wu, R. Purcell, C. Querner, M. Drndic, M. Pelton, *Nano Lett.* **2010**, *10*, 1692.
[34] W. Xu, W. Liu, J. F. Schmidt, W. Zhao, X. Lu, T. Raab, C. Diederichs, W. Gao, D. V. Seletskiy, Q. Xiong, *Nature* **2017**, *541*, 62.
[35] J. Zhou, M. Zhu, R. Meng, H. Qin, X. Peng, *J. Am. Chem. Soc.* **2017**, *139*, 16556.
[36] A. Zhang, C. Dong, H. Liu, J. Ren, *J. Phys. Chem. C* **2013**, *117*, 24592.
[37] D. E. Gomez, J. van Embden, J. Jasieniak, T. A. Smith, P. Mulvaney, *Small* **2006**, *2*, 204.
[38] G. Ramakrishna, H. N. Ghosh, *Langmuir* **2003**, *19*, 3006.
[39] C. N. Valdez, A. M. Schimpf, D. R. Gamelin, J. M. Mayer, *ACS Nano* **2014**, *8*, 9463.
[40] W. Lin, J. Walter, A. Burger, H. Maid, A. Hirsch, W. Peukert, D. Segets, *Chem. Mater.* **2015**, *27*, 358.
[41] A. Sasidharan, P. Chandran, D. Menon, S. Raman, S. Nair, M. Koyakutty, *Nanoscale* **2011**, *3*, 3657.
[42] P. A. Nikitina, A. S. Peregudov, T. Y. Koldaeva, L. G. Adiulin Kuz'mina, E. I. Tkach, V. P. Perevalov, *Tetrahedron* **2015**, *71*, 5217.
[43] N. Komiya, M. Okada, K. Fukumoto, D. Jomori, T. Naota, *J. Am. Chem. Soc.* **2011**, *133*, 6493.

© 2018 WILEY-VCH Verlag GmbH & Co. KGaA, Weinheim